Polarization-locked VCSEL with PM fiber pigtail for quantum communication

Guofeng Xin (辛国锋)[*]**, Li Shen (沈 力), Haoyang Pi (皮浩洋), Dijun Chen (陈迪俊), Haiwen Cai (蔡海文),**
Huizhong Feng (封惠忠), Jianxin Geng (耿健新), Ronghui Qu (瞿荣辉), Gaoting Chen (陈高庭),
Zujie Fang (方祖捷), and Weibiao Chen (陈卫标)

Shanghai Institute of Optics and Fine Mechanics, Chinese Academy of Sciences,

Shanghai Key Laboratory of All-Solid State Laser and Applied Techniques, Shanghai 201800, China

[*]*Corresponding author: gfxin@siom.ac.cn*

Received March 30, 2012; accepted May 17, 2012; posted online August 16, 2012

Quantum communication is a new technology requiring a stable and reliable laser source for communication security. A new kind of polarization-locked vertical-cavity surface-emitting laser (VCSEL) with polarization maintaining (PM) fiber pigtail is fabricated as a decoy state laser source. The VCSEL is packaged in a standard butterfly box integrated with thermoelectric coder (TEC) and thermistor. The optical pulse width of full-width at half-maximum (FWHM) is smaller than 400 ps with a 100-MHz on/off modulation frequency. The results reveal that modulation range is better than 4. Moreover, the polarization is stable, and the power extinction ratio is larger than 25. The center wavelength is 850 nm, and the SMSR is better than 40 dB.

OCIS codes: 140.3325, 140.7260, 230.0250.

doi: 10.3788/COL201210.101403.

Quantum communication has become the focus of various studies in recent years due to its ability to realize the absolute security of secure communication, quantum teleportation, and quantum dense coding, among other. Research groups have achieved long-distance quantum communication using different methods[1−3]. However, there are few lasers, such as single photon, continuously exhibit variable and entangled state sources[4,5]. Quantum communication requires decoy state laser source with stable polarization, faster rise/fall speed, single longitudinal and transverse modes, and larger modulation range[6] with on/off electrical pulse pumping that is different from classical communication with sine or square pulse modulation.

The commercial single photon detector (SPD) wavelength currently used in quantum communication has limited functions in short wavelengths near the infrared (IR), such as at a wavelength of 850 nm. Although the distributed feedback (DFB) laser diodes have faster modulation speed, their wavelengths are almost at 1 310 and 1 550 nm. The wavelength of Fabry-Perot (FP) laser diodes is 850 nm, but their rise/fall time is larger than 1 ns. The rise/fall time of the vertical-cavity surface-emitting laser (VCSEL) chip with TO or butterfly packaging is smaller than 500 ps. However, the commercial products of VCSEL are almost in multi-transverse mode, and their polarizations are unstable when the driving current changes. In addition, VCSEL has less laser module that satisfies all of the requirements of the laser source for quantum communication. Nevertheless, a laser source based on semiconductor optical amplifiers has been proposed in Ref. [7].

In this letter, the polarization-locked VCSEL chip, the Panda polarization maintaining (PM) fiber, the thermoelectric cooler (TEC), and the thermistor are integrated without glue in a standard high-speed butterfly box. The fiber feedthrough is sealed with solder and the lid is sealed by a parallel sealer for higher reliability. The power stabilities under continuous waves (CWs) at different TEC set temperature and ambient temperature current pumping are also given. Finally, the characteristics of the module are tested with pulse electrical pumping.

The VCSEL is polarization locked with integrated grating on the chip surface. The radius of the aperture was about 2.7 μm. The chip of the VCSEL (Oclaro, Inc.) (Fig. 1(a)) was very similar in structure to the one reported in Ref. [8]. Polarization locking technology was also introduced in Ref. [9], but its characteristics and process technologies are different from those of high-power VCSEL[10,11].

To obtain the electrical connection, the VCSEL chip was soldered on gold coated-AlN and gold wire was bonded on the side. The AlN with laser chip, the TEC, the thermistor, and the metal plate for fixing the metalized fiber module by laser welding were soldered together in the standard butterfly box. The fast or slow axis of the Panda PM fiber was aligned directly to the polarization direction of the VCSEL chip without any lens. The metalized fiber module was then fixed onto the metal plate using pulse laser welding.

The polarization extinction ratio (power) tested block diagram was given under a CW current pumping (Fig. 2); the laser module was pumped by a CW current source.
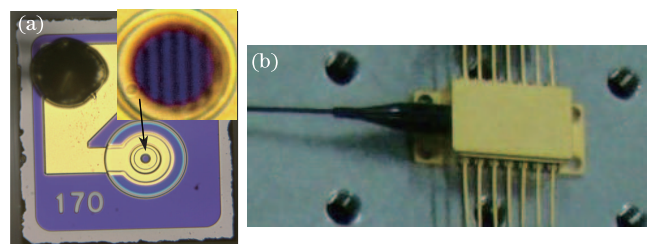

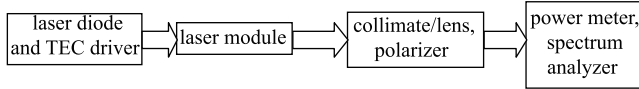Fig. 1. (a) VCSEL chip; (b) packaged laser module.

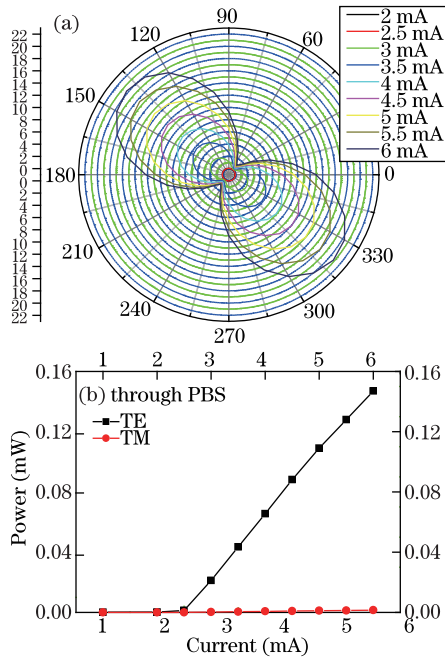Fig. 2. Tested block diagram with CW current pumping.

Fig. 3. (a) Polarization measurement results; (b) power versus current.

The laser was collimated by an aspheric lens and went through a polarizer (100 000:1). The polarizer was then turned to 360°. The maximum and minimum power levels were detected by the power meter, from which the polarization extinction ratio (PER, Pmax/Pmin) was calculated. The spectrum was tested directly by the spectrum analyzer with 0.01-nm resolution. The device was placed in the temperature cycle oven to change the ambient temperature. The power was detected by the power meter.

The width of the optical pulses pumped by the electrical pulse source (pulse width of 200 ps) was measured by a high-speed oscilloscope (6 GHz) and a high-speed optical detector (frequency range of 5 GHz, responsibility of 1.1 V/mW, wavelength ranges from 500 to 870 nm).

Next, we measured the polarization of the VCSEL. Results are given in Fig. 3(a), which explains the better polarization stability of the device and the extinction ratio with increased current. Figure 3(b), meanwhile, explains the power versus current relationship, wherein transverse electrical (TE) and transverse magnetical (TM) indicate different polarization directions. No polarization jump is observed with current increase, such as in other VCSELs[12].

The PER (Pmax/Pmin) of different laser modules tested at 3.5-mA current are larger than 25. The PER is mainly influenced by the aligned accuracy between the fast/slow axes of the PM fiber and the VCSEL chip, and the feedthrough was sealed with solder. Results are given in Table 1.

Figure 4 shows the typical P-I and V-I plots as well as the spectra and wavelengths that change with the current. The power is 441 μW at 4.5 mA with a coupling

efficiency of about 25%. The threshold current is about 2 mA, the differential resistance is less than 65 Ω, and the slope efficiency is 0.189 mW/mA. The center wavelength is 850.206 nm at 4.0 mA, the SMSR is larger than 40 dB; the wavelength coefficients with current and temperature are approximately 0.229 nm/mA and 0.06 nm/°C, respectively.

Power is detected when the TEC setting temperatures change from 22 to 28 °C (Fig. 5(a)). This result indicates that the power coefficient with temperature is 1.58 μW/°C; moreover, the power increases with temperature, which reverses to a high power laser diode without fiber coupling. The module power changes along with variations in ambient temperature (Fig. 5 (b)), although the temperature of TEC is 25 °C. The wavelength only varies by 0.00375 nm with the ambient temperature ranging from 30 to 20 °C. This phenomenon has also been reported in Ref. [13]. Figure 5(c) provides that chip temperature only changes by 0.0625 °C. Given that this slightly influences the optical power of the chip, it is assumed that others factors causes power to change with temperature. This shall be studied in the future using theoretical simulation and experiments.

Table 1. Polarization Extinction Ratios of Different Laser Modules

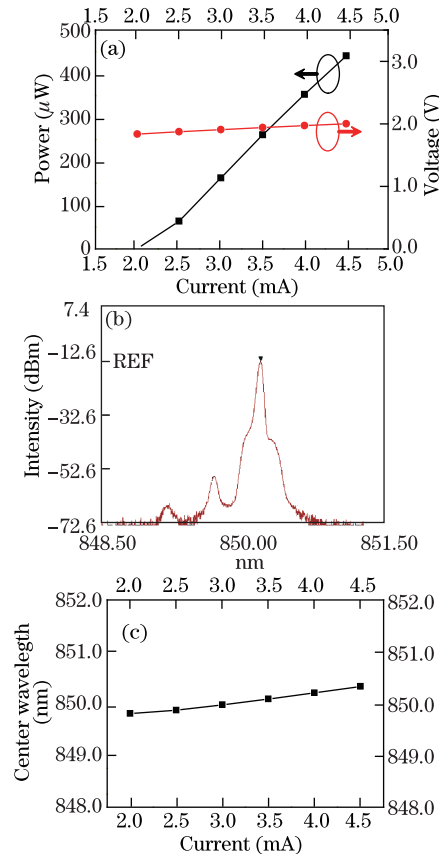| No.	1	2	3	4	5	6	7
PER@3.5 mA	138.9	190.1	120	290	82.5	25.2	38

Fig. 4. (a) Power and voltage versus current curves; (b) spectrum at 3.5-mA CW current; (c) center wavelength versus current.
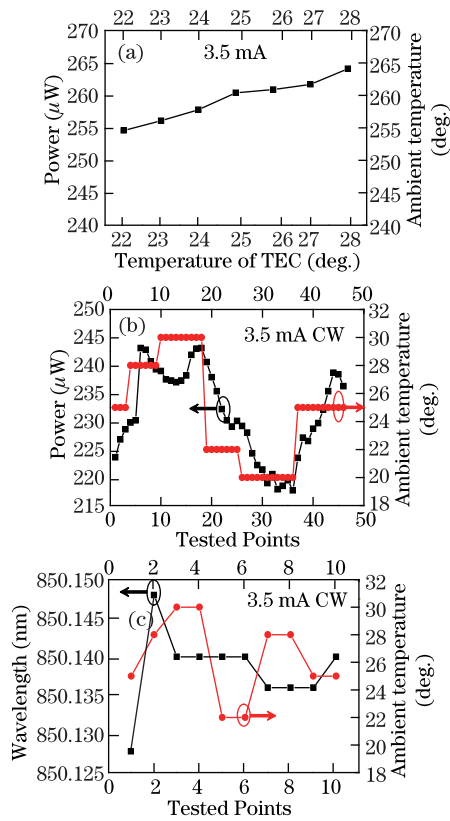
Fig. 5. (a) Power changes with TEC temperature; (b) power changes with environment temperature at 3.5 mA and TEC setting at 25 °C; (c) wavelength changes with ambient temperature.
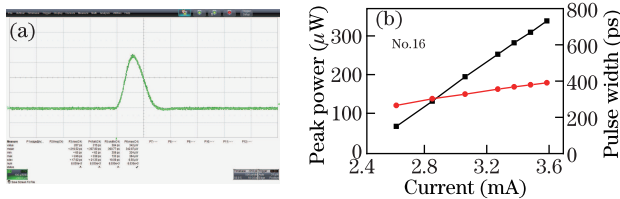

Fig. 6. (a) Optical pulse; (b) power and pulse width versus pulse current.

Table 2. Modulation Ratios of Different Laser Modules

No.	1	2	3	4	5	6	7
Modulation Ratio	4.28	4.13	4.68	4.27	4.52	4.88	4.608

After performing the experiment under the CW current, the module is pumped on/off by high-speed pulse current source with 200-ps electrical pulse. The optical pulse is provided in Fig. 6, which indicates that the pulse width is smaller than 400 ps. The peak power of 390 μW can be attributed to detector saturation at the 1.0-mW peak power, which attenuates the power in the testing

process. Figure 6 shows the peak power after attenuation; it also shows that the pulse width changes with the current, indicating that the peak power is linear with the pumped current, and the pulse width is smaller than 400 ps. Modulation is defined as the power at higher current compared with lower current. The result is presented with different modules in Table 2, which shows that the modulation is larger than 4 and can be applied in quantum communication.

In conclusion, in this letter, we present the fabrication of a new kind of polarization-locked VCSEL module with PM fiber pigtails. It shows stable polarization with an optical pulse smaller than 400 ps with better modulation range. Power stability with temperature is also studied experimentally. In future works, we aim to improve coupling efficiency and stability without reducing the modulation characteristics.

References

1. S. Wang, W. Chen, J.-F. Guo, Z.-Q. Yin, H.-W. Li, Z. Zhou, -C. Guo, and Z.-F. Han, Opt. Lett. **37,** 1008 (2012).
2. Z. Feng, Z. Jun, and Z. Guihua, J. Nanjing University of Posts and Telecommunications (in Chinese) **31,** 83 (2011).
3. Q. Wang, X.-B. Wang, and G.-C. Guo, Phys. Rev. A **75,** 012312 (2007).
4. C.-Z. Peng, J. Zhang, D. Yang, W.-B. Gao, H.-X. Ma, H. Yin, H.-P. Zeng, T. Yang, X.-B. Wang, and J.-W. Pan, Phys. Rev. Lett. **98,** 010505 (2007).
5. A. Scherer, B. C. Sanders, and W. Tittel, Opt. Express **19,** 3004 (2011).
6. X. Wang, http://arxiv.org/abs/quant-ph/0411047v5.
7. M. Jofre, A. Gardelein, and G. Anzolin, Opt. Express **19,** 3825 (2011).
8. J. M. Ostermann, P. Debernaridi, C. Jalics, A. Kroner, M. Feneberg, M. C Riedl, and R. Michalzik, Proc. SPIE **5364,** 201 (2004).
9. Z. Rao, S. Vo, and J. S Harris, Chin. Opt. Lett. **6,** 748 (2008).
10. L. Hou, G. Zhong, and Y. Zhao, Chin. Opt. Lett. **7,** 709 (2009).
11. C. Yan, G. Lu, and L. Qin, Chin. Opt. Lett. **8,** 595 (2010).
12. A. Valle, L. Pesquera, and K. A. Shore, IEEE Photon. Technol. Lett. **10,** 639 (1998).
13. J. Barbero, D. Lopez, I. Esquivias, J. M. G. Tijero, and M. Fischer, in *Proceedings of International Conference on Space Optics ICSO* (2010).